Original research or treatment paper

Salt efflorescence on pottery in the Athenian Agora: A closer look

Alice Boccia Paterakis[1], Michael Steiger[2]

[1]Japanese Institute of Anatolian Archaeology, Kaman, Turkey, [2]Department of Chemistry, University of Hamburg, Hamburg, Germany

Salt contamination in the ceramic collection of the Athenian Agora, American School of Classical Studies, Greece, was confronted for the first time by the fulltime conservation staff that was appointed in 1979. A review is presented of the examination and analysis of the salt contaminants for their identification and of simulation tests to determine their source(s) and mode of formation since 1990. In the analytical campaigns of 1992 and 1994, calclacite ($Ca(CH_3COO)Cl \cdot 5H_2O$) (ICCD 12-0869) and calcium acetate hemihydrate ($Ca(CH_3COO)_2 \cdot 0.5H_2O$) (ICCD 19-0199) were identified with X-ray diffraction and polarized light microscopy and examined with the environmental scanning electron microscope. The various means with which to mitigate the contamination and the crystallization-deliquescence cycles, e.g. consolidation, desalination, and climate control, were also studied. The article focuses on the processes involved in the formation of acetate salt compounds with the publication of the first solubility and deliquescence diagrams of the $Ca(CH_3COO)_2–CaCl_2–H_2O$ system at 25°C. Comparisons are drawn with recent work carried out on thecotrichite ($Ca_3(CH_3COO)_3Cl(NO_3)_2 \cdot 7H_2O$). The course of action adopted by the conservation staff of the Athenian Agora to combat efflorescence has been termination of cleaning with hydrochloric acid and desalination as a remedial measure *in lieu* of the costly replacement of wooden cabinets with enameled steel storage cases for the extensive ceramic collection (52,000 catalogued ceramics). Volatile acetic acid concentrations in wooden storage cases in the collection have been found to range from 1039 ± 20 to $1267 \pm 20 \ \mu g/m^3$ (400 to 500 ppb) at 25°C. Since 1979, all newly excavated ceramics and all ceramics exhibiting efflorescence in the collection have been routinely desalinated. No efflorescence has formed on the desalinated objects. Various methods of mitigation such as controlling the RH are also discussed.

Keywords: Volatile organic compounds, Acetic acid, Ceramic, Pottery, Desalination, Salts, Calclacite, Calcium acetate hemihydrate

Introduction

One of the earliest references to the deterioration of inorganic materials by the effects of volatile carbonyl compounds was published in 1899 dealing with the corrosive effects of acetic acid on shell (Byne, 1899). This was followed in 1923 and 1926 with publications on the efflorescence on limestone in the British Museum (Scott, 1926). Calcium acetate efflorescence was identified on mineral specimens in 1931 (Taboury, 1931). Calclacite, calcium acetate chloride pentahydrate ($Ca(CH_3COO)Cl \cdot 5H_2O$), was identified on calcareous rocks in Brussels in 1945 that were stored in oak cases (Van Tassel, 1945; Van Tassel, 1958).

The effects of volatile acetic acid on ceramics that were first noted were calclacite crystals on a Babylonian baked clay cone in the Semitic Museum of Harvard University in 1948 (Fitzhugh & Gettens, 1971). Calclacite was found on two Greek vases in the Fogg Museum in 1950 and on ceramics from Ur in the British Museum in 1960 (Fitzhugh & Gettens, 1971). In 1993 calclacite was identified on a Greek ceramic in the Metropolitan Museum of Art, New York (Wheeler & Wypyski, 1993). Calclacite was identified on a Cypriot vase in the Ashmolean Museum (Halsberghe *et al.*, 2005a). All the ceramics in question had been stored in wooden cases.

The pottery collection in the Athenian Agora displayed considerable salt contamination evidenced by efflorescence in uncontrolled climatic conditions. Until 1979 pottery excavated in the Athenian Agora was routinely cleaned in hydrochloric acid to remove calcium carbonate encrustations without presoaking in water and without rinsing with water afterward (Koob, 2013). This introduced acid that reacted with calcium carbonate forming calcium chloride in the ceramic matrix. These ceramics containing calcium

Correspondence to: Alice Boccia Paterakis, 23835 Arroyo Park Drive, #1104, Valencia, CA 91355, USA. Email: Alice.Paterakis@Scrippscollege.edu or alicepaterakis@yahoo.com

chloride were subjected to volatile acetic acid emissions in wooden storage cabinets for many years. Soil from burial is another source of chloride contamination. Desalination of the ceramic collection commenced in 1979 when the first professionally trained, full time conservator hired on staff determined that the salts were water-soluble. Soluble salts in pottery exert destructive forces through crystallization that can dislodge glaze on the surface interfering with the legibility of the object and cause loss of information (Fig. 1A). Internal crystallization can lead to the physical disruption of the ceramic body resulting in complete fracturing and loss of the whole (Fig. 1B). Efflorescence can be so dense as to completely obscure an object (Fig. 1C).

The first analysis of the efflorescence to be carried out identified calclacite and an unidentified compound, using neutron activation analysis (NAA) and X-ray diffraction (XRD) (Paterakis, 1990). The challenges of desalinating extensively deteriorated ceramics were addressed by carrying out consolidation and desalination simulation tests using tetraethyl orthosilicate (TEOS), methyl triethoxysilane (MTS), and Paraloid® B-72 in a calcareous and non-calcareous ceramic. Based on the analytical results of 1990, calcium acetate was selected as a salt contaminant in these tests (Paterakis, 1993), as was sodium sulphate (Paterakis, 1992) and sodium chloride (Paterakis, 1998a). The ceramic test tiles were impregnated with the salt solution (1.5 M concentration) prior to their consolidation. The desalination methods tested were static immersion and stirred solution. All three consolidants allowed the dissolution of the salt and its removal by desalination with little variance in efficiency between the two desalination methods tested. Accelerated efflorescence tests were conducted to monitor the passage of water through the consolidated, salt-laden ceramics (Paterakis, 1995). All three consolidants protected the ceramic fabric from physical damage while allowing salt to migrate to the surface and crystallize.

Paraloid® B-72 was rarely used to consolidate pottery from 1979 to 1985. Based on the degree of success achieved with Paraloid® B-72 in the consolidation tests previously discussed it was decided to use Paraloid® B-72 to strengthen those Agora ceramics most severely weakened by salt crystallization to enable desalination. Paraloid® B-72 is also highly recommended as an adhesive for the reconstruction of pottery vessels (Koob, 1986). While TEOS and MTS performed well, as consolidants they are recommended only when reversible materials are not available on account of their irreversible nature. Since 1993 only the most friable ceramics in the collection have been

Figure 1 Salt efflorescence on pottery in the Athenian Agora: (A) loss of surface by soluble salt crystallization (image is 7 cm across), (B) internal disruption of amphora neck by soluble salt crystallization, (C) needle-like crystals on lamp in wooden storage drawer, (D) snowflake crystal formations on lamp.

consolidated with a solution of Paraloid® B-72 and ethanol/acetone of varying concentration and solvent ratio by spraying, brushing, or immersion. The application method was dictated by the condition of the ceramic. The consolidant was sprayed onto those objects in storage that were too fragile to be moved. Once strengthened by the consolidant, they were moved from storage to the conservation laboratory where desalination was carried out by immersion. While consolidation with Paraloid® B-72 slows down the rate of salt removal, desalination may be successfully achieved. Poulticing is another viable method of desalination.

In order to understand the source and formation of these salts, and to prevent their continued occurrence in the collection, it was necessary to carry out

further testing and analysis. In 1992 and 1994 analytical campaigns using polarized light microscopy (PLM), environmental scanning electron microscopy (ESEM), and XRD were performed to aid in the characterization of the salts. Salt efflorescence on 14 ceramic objects including a skyphos, two official measures, and several lamps was sampled in 1991 (Table 1). These ceramics were excavated between the years 1931 and 1948; analysis was carried out 43–60 years following their excavation. These objects had been stored in wooden drawers and cabinets in uncontrolled climatic conditions since their excavation.

To test the hypothesis for the formation of calcium acetate on calcareous ceramics from the reaction with volatile acetic acid, accelerated efflorescence tests were carried out (Paterakis, 1995). These simulation tests exposed a calcareous and a non-calcareous ceramic, with and without sodium chloride and hydrochloric acid contaminant, to volatile acetic acid in a wind tunnel. Salt efflorescence based on calcium acetate formed on the surface of all the calcareous ceramic test tiles (identification by infrared spectroscopy and XRD) whereas it did not form on the non-calcareous ceramic (Paterakis, 1995). The calcareous component represented 6.36–8.77% weight as calcium carbonate and amphibole in the test pieces confirming that calcium in pottery does contribute to the formation of calcium acetate compounds when subjected to volatile acetic acid (Paterakis, 1995).

The experimental design and results of the analytical campaign involving XRD, ESEM, and PLM from 1992 and 1994 are reported in the following sections as they delve into the salt contaminants in the Athenian Agora in greater detail. The analytical results of the salts are discussed in the subsequent section in terms of their formation as illustrated by the first publication of the phase diagram of the $Ca(CH_3COO)_2$–$CaCl_2$–H_2O system at 25°C.

Experimental design

XRD was performed on salt efflorescence from fourteen ceramic objects (Table 1). The samples were mounted with Paraloid® B-72 acrylic resin in acetone to a 0.1-mm Mark-Röhrchen glass spindle and placed in a circular Rigaku diffraction camera. Samples were run at 30 mA and 40 kV with a nickel filter in a Rigaku Geigerflex X-ray diffractometer. The resulting XRD patterns were identified with the Powder Diffraction file. PLM was carried out on an Orthoplan-Pol polarizing light microscope. The PLM and XRD were carried out in the J. Paul Getty Antiquities Laboratory in 1992 (Mau, 1992). ESEM was performed with an Electroscan E3 using 20 keV at 2 Torr water vapor pressure in the SEM laboratory

Table 1   Ceramics analyzed

Getty sample no.	Agora inv. no.	Description	Date excavated	Salt form
1	P18420	4th c. BC Greek black glaze skyphos	1947	Needle
2	L4464	1st c. AD Greek lamp with glaze wash	1948	Needle
3	P8098	5th c. BC Greek black glaze official measure	1936	Snow-flake
4	L4885	Roman lamp with red-brown glaze	1937	Needle
5	L346	Greek lamp with thin glaze	1932	Needle
6	SS6593	Greek stamped public pot handle with thin wash	1936	Needle
7	P5905a	Greek black figure official measure fragment	1935	Needle
8	L208	Roman unglazed lamp	1931	Snow-flake
9	L4071	Roman unglazed lamp	1940	Snow-flake
10	PN L181	Lamp with red glaze	1932	Needle
11	PN P280	Mould fragment for Megarian bowl	1934	Needle
12	PN P324	Mould fragment for Megarian bowl	1934	Needle
13	PN L177	Lamp with red glaze	1934	Needle
14	PN L248	Lamp with black glaze	1937	Needle

of the Getty Conservation Institute in 1994 (Doehne, 1994).

Results

X-ray diffraction

Calclacite (JCPDS 12-0869) was identified as the major component of 12 of the 14 samples with major diffraction lines at 2.43 Å, 3.24 Å, and 8.27 Å (Table 2). In most samples the presence of quartz was suggested by a diffraction line at 3.34 Å. Quartz was identified as the major component in samples 8 and 9, with lesser amounts of calclacite. Sample 12 contained approximately equal amounts of quartz and calclacite.

During sampling the efflorescence was distinguished with the naked eye as needle-like (Fig. 1C) or snow-flake-like (Fig. 1D). Under low magnification, many of the samples appeared to consist of a snowy, granular compound and transparent, needle-shaped crystals. These two morphologies were separated in samples 4, 6, and 7 and analyzed by XRD independently. In all cases, however, both morphologies gave patterns for calclacite.

Several samples contained one or more compounds in addition to calclacite and quartz. The XRD pattern for samples 8, 9, and 11 identified the presence of calcium acetate hemihydrate ($Ca(CH_3COO)_2 \cdot 0.5H_2O$) ICCD 19-0199 (Table 3). This compound was tentatively identified as a minor component in sample 2 (Table 2).

In some cases preliminary results required confirmation by running the samples more than once. Calcium acetate hemihydrate was indicated primarily in the first run for sample 4 (film 276). Subsequent patterns (film 313, 314) identified only quartz and calclacite that may be explained by non-representative sampling. The preliminary analysis of sample 11 (film 268) identified calclacite and quartz with an unidentified minor component. A second run (film 271) identified calcium acetate hemihydrate as the minor component. Once again, the discrepancy between the patterns may be the result of non-representative sampling.

Polarized light microscopy

The results of PLM confirmed calclacite but were not conclusive regarding the minor component(s) (Table 4). The acicular form of calclacite was characterized (Van Tassel, 1958) and calcium acetate hemihydrate in sample 11 was tentatively identified. Quartz was identified and the relative amounts were determined in the samples.

The acicular needles of calclacite are transparent and smooth with squared off ends (Fig. 2A). Similar calclacite needles from a Cypriot vase in the Ashmolean Museum were detected with light microscopy (Halsberghe *et al.*, 2005b). The acicular needles have a refractive index <1.66 and medium relief in 1.66 Cargille Meltmount™. These crystals are weakly birefringent and give a blue-white coloration in crossed polarizers. A negative sign of elongation was determined using a first order red compensator in crossed polarizers.

Weakly birefringent and irregularly shaped particles of 2–5 μm made up the bulk of the samples. These particles were found as agglomerations of distinctly rectangular forms (Fig. 2B), worm-like (vermiform) shapes (Fig. 2C), or undefined clusters (Fig. 2D). These clusters are considered to be finely ground samples of calclacite since they appear in all the samples that have been identified as calclacite. Perhaps these resulted from mechanical damage to the crystals during sampling. The agglomerated particles in rectangular groups were found to have a positive sign of elongation with respect to the long side of the agglomeration, in contrast to the acicular calclacite needles (both rectangular agglomerations and needles appear in Fig. 2E).

The particles in sample 11 that were identified as calcium acetate hemihydrate by XRD differed from the acicular needles of calclacite by their ragged edges and node-like swellings (Fig. 2F). They had a refractive index <1.66 and showed a weaker

Table 2   Results of XRD analysis

Sample no.	Film no.	Calclacite	Calcium acetate hemi-hydrate	Unidentified minor compound
1	315	X		
2	280	X	X	
3	306	X		
4	276		X	
	313 needles	X		
	314 granular	X		
5	275	X		
	311	X		X
6	300 needles	X		
	302 granular	X		
7	303 needles	X		
	304	X		
	305	?		
8	291	X	X	
	292	X	X	
9	312	X	X	
10	299	X		
11	268	X		X
	271	X	X	
12	307	X		
13	308	X		
14	309	X		

Table 3   XRD pattern for sample 8

Sample 8 (film 291)		Calclacite Ca(CH₃COO)Cl·5H₂O JCPDS 12-0869		Calcium acetate hemihydrate Ca(CH₃COO)₂·0.5H₂O ICCD 19-0199	
d-spacing	Intensity	d-spacing	Intensity	d-spacing	Intensity
13.262	100			16.7	75
11.065	30			11.7	100
8.311	80	8.27	100	8.4	65
7.020	40	6.87	75	6.98	16
6.130	80	6.15	50		
5.697	30			5.57	30
4.215	20	4.16	75	4.18	10
3.663	10	3.67	50	3.66	4
3.443	50			3.52	30
3.322	90	3.24	100	3.35	25
3.039	50	3.06	50	3.02	10
2.690	10	2.65	50	2.68	8
2.572	10			2.56	10
2.439	30	2.43	100	2.39	12
2.299	20	2.3	75	2.28	8
2.207	20	2.22	50	2.18	6
2.105	5	2.14	50	2.14	12
2.035	20	2.04	75	2.06	8
1.888	5	1.876	25	1.86	8

birefringence than calclacite. Notably, their sign of elongation was positive, opposite that of calclacite (calclacite and this other compound form an 'X' in Fig. 2G).

It is important to note that there were ragged, needle-shaped particles also with a negative sign of elongation (Fig. 2H) as well as ragged and smooth crystals that changed sign of elongation (Fig. 2G).

These inconsistencies suggest chemical changes taking place in the crystals, such as the hydration state of the compound. Further research is called for to resolve these questions.

Environmental scanning electron microscopy
Sample 3 was examined at magnifications from 20× to 20,000× with the ESEM (Doehne, 1994). PLM of this

Table 4   Results of polarized light microscopy

Sample no.	Calclacite needles	Quartz	Agglomerations			Non-Agglomerated vermiform (ragged)
			Rectangular	Vermiform	Undefined	
1	10		50		40	
2	50	15		35		
3		20			80	
4	5	10	30		55	2
5	10	5	45		40	
6	30	10		35	15	10
7	5	20	45	10	20 (coating quartz)	
8		80			20 (coating quartz)	
9		50			50	
10		2	50		40	
11	40	10				50
12						
13		2	20	8	70	
14	30	5		65		

Numbers represent approximate percentage weight fractions within each sample.
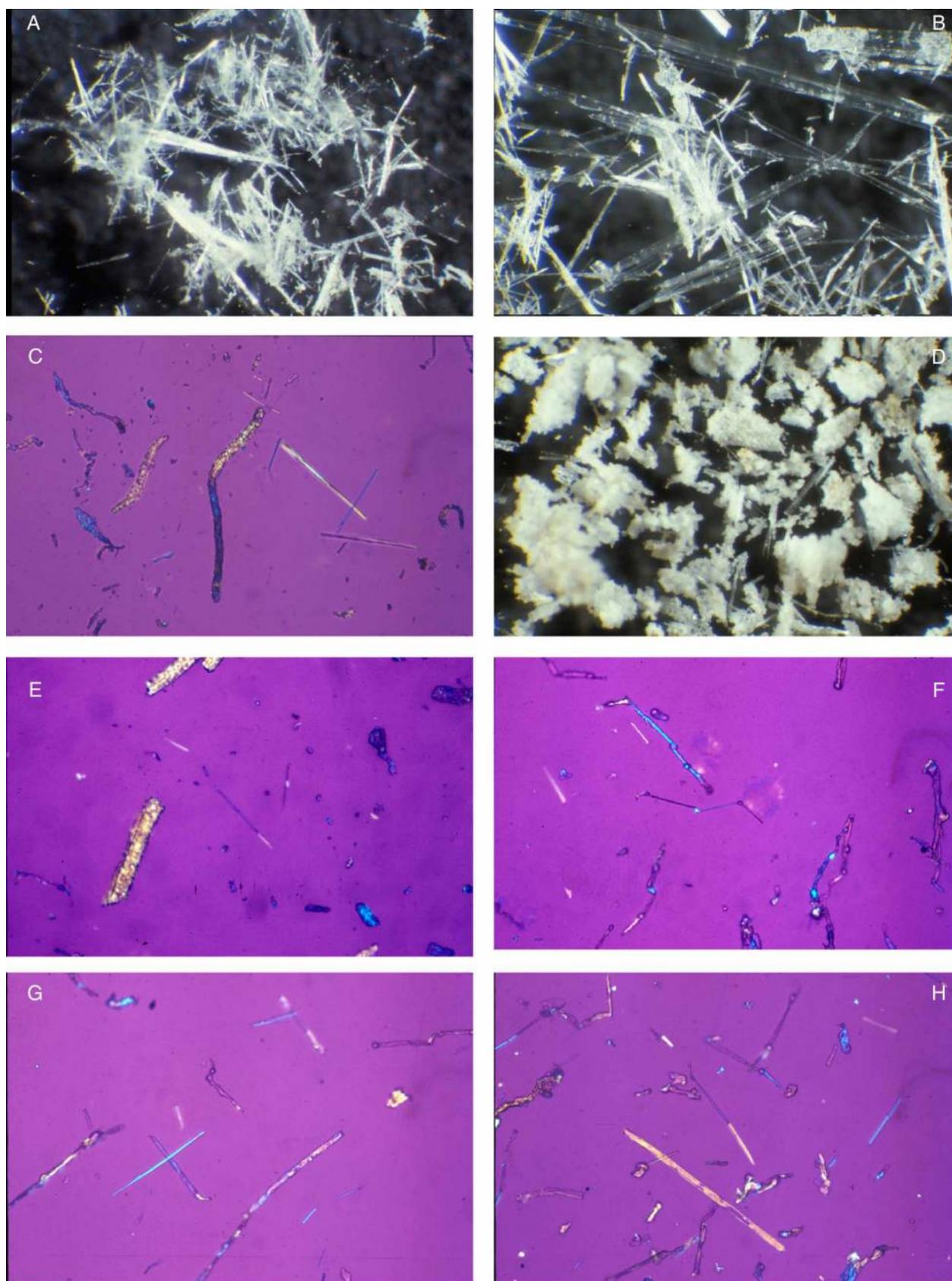
Figure 2   PLM micrographs: (A) acicular calclacite (image is 4.4 mm across), (B) rectangular forms (image is 4.4 mm across), (C) vermiform shapes, $\lambda/4$ wave compensator, 1.66 Cargille (image is 0.55 mm across), (D) similar undefined clusters in Fig. 5Ac of Stahlbuhk, 2012 (calclacite and calcium acetate hemihydrate on third century BCE Near Eastern clay tablet stored in wood from the Museum of the Ancient Near East, Berlin) (image is 340 μm across), (E) both needles and rectangular agglomerations are present, $\lambda/4$ wave compensator, 1.66 Cargille (image is 0.55 mm across), (F) calcium acetate hemihydrate needles with nodes, $\lambda/4$ wave compensator, 1.66 Cargille (image is 0.55 mm across), (G) calclacite with calcium acetate hemihydrate, $\lambda/4$ wave compensator, 1.66 Cargille (image is 0.55 mm across), (H) needles with negative sign of elongation, $\lambda/4$ wave compensator, 1.66 Cargille (image is 0.55 mm across).
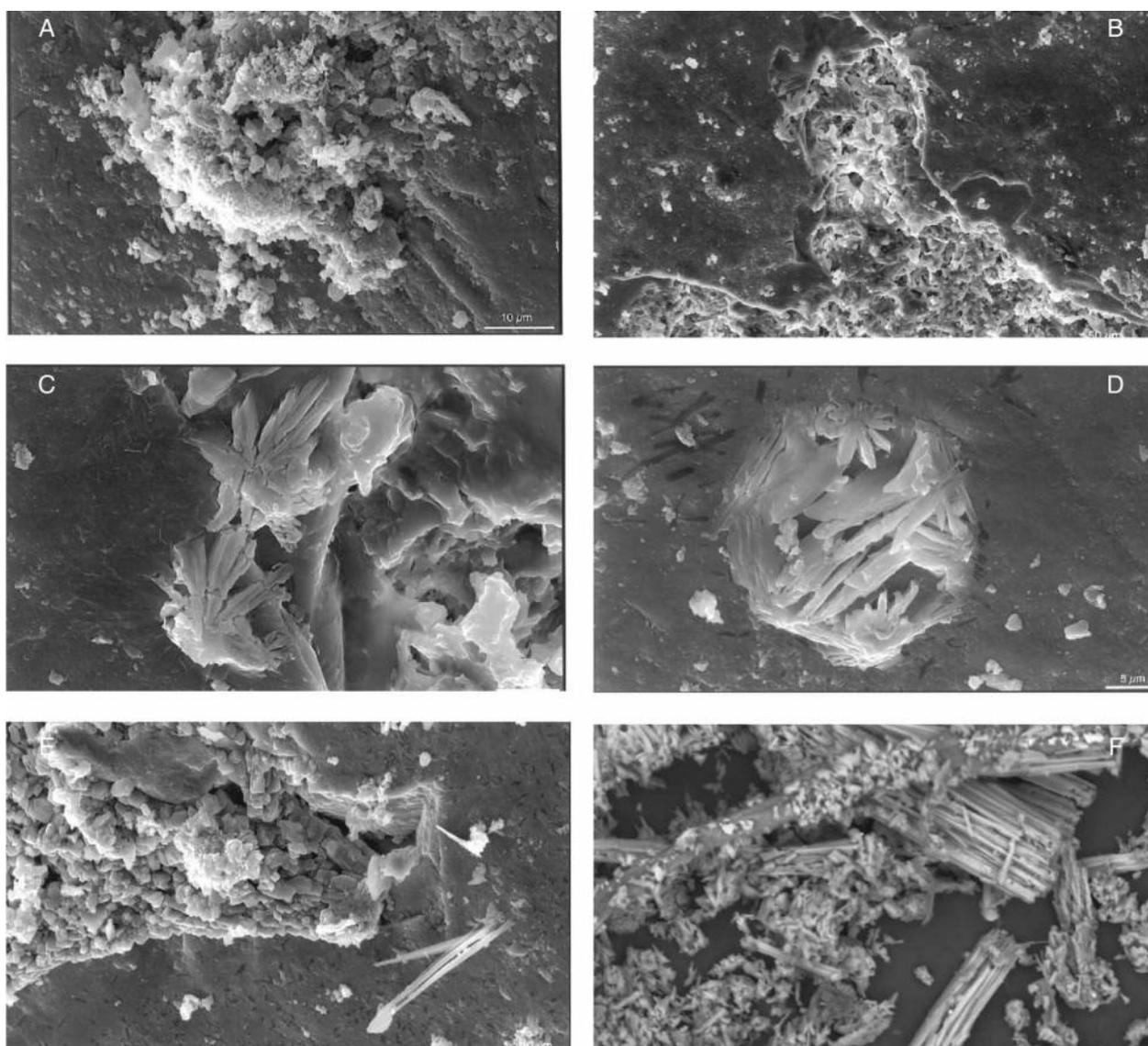
Figure 3 SEM micrographs. (A) salt accumulation on surface of the black glaze (image is 80 μm across), (B) salt crystals underneath the black glaze (image is 250 μm across), (C) (detail of Fig. 3b), note snowflake morphology of crystals at edge of fractured black glaze (image is 40 μm across), (D) round blister has erupted through the black glaze surface filled with long, rectangular grains as well as crystals resembling droplets or snowflakes at the edges of the blister. Note small dark crystals on surface of black glaze (image is 51 μm across), (E) three crystal morphologies: equant grains in the left and center, needle-like crystals on the right, and smaller dark crystals lying on the smooth surface of the black glaze (image is 107 μm across), (F) scanning electron micrograph of calclacite and calcium acetate hemihydrate (sample 6a) from another third century BCE Near Eastern clay tablet that was stored in wood from the Museum of the Ancient Near East in Berlin (Fig. 13 in Stahlbuhk, 2012) (image is 300 μm across).

sample removed from the surface of the ceramic revealed predominantly undefined agglomerations (Table 4) that were identified as calclacite with XRD (Table 2). Sixteen digital secondary electron micrographs were taken of sample 3 with the ESEM. The ESEM was able to distinguish different crystal morphologies according to location of the salts: on the surface of the black glaze (Fig. 3A), underneath the black glaze (Figs. 3B, C), and in pores caused by eruption of salt blisters through the surface of the glaze (Fig. 3D). The crystals at the edges of the fractured black glaze in Fig. 3C reveal a snowflake or droplet morphology. These snowflake crystal formations in

Figs. 3C and D appear to be stellated polygons, perhaps with nine points although this is difficult to determine. Parallels for this morphology have not been found in the literature except for reference to a star shape formation of sodium calcium formate around a sodium formate anhydrate nucleus on glass objects in the National Museums of Scotland (Robinet *et al.*, 2004). Three crystal morphologies are present in Fig. 3E, equant grains in the left and center, needle-like crystals on the right, and rectangular dark crystals lying on the smooth surface of the black glaze. The round blister that has erupted through the black glaze surface in Fig. 3D is filled

with long, rectangular grains as well as stellated polygons at the edges of the blister. Again dark crystals can be seen on the surface of the black glaze surrounding the blister. The lighter and darker needles may be different crystalline forms of calclacite (Doehne, 1994). A mixture of calclacite and calcium acetate hemihydrate identified on another third-century BCE Near Eastern clay tablet that was stored in wood from the Museum of the Ancient Near East in Berlin reveals a combination of rectangular crystals and undefined clusters in the SEM (Fig. 3F) (Stahlbuhk, 2012).

The ESEM examination correlates well with the examination by PLM with regard to those salts sampled from the surface of the object: more than one crystal morphology was detected. The four crystal morphologies (equant, needle-like, rectangular, and snowflake) observed with the ESEM in sample 3 are supported by the various salt crystallization morphologies for one salt compound detected by Zehnder and Arnold (Zehnder & Arnold, 1989; Arnold & Zehnder, 1991). The discovery of three morphologies of sodium formate on glass, i.e. round, large/flat, and needle-like crystals, further confirms the multiple morphological states of salts (Robinet et al., 2004).

In conclusion, XRD identified most of the samples as calclacite with quartz present. The quartz crystals were dislodged from the fabric during the crystallization of calclacite and calcium acetate hemihydrate in the outermost pores of the ceramic as a result of mechanical damage (the solubility of quartz is too low for leaching to take place). Minor amounts of other compounds such as calcium acetate hemihydrate were identified in several samples. PLM was able to identify and characterize calclacite. PLM confirmed the presence of quartz in varying amounts in the samples. Although physical and chemical changes can occur during the storage of the samples and their mounting for XRD and PLM, since acetates are not hygroscopic and the salt samples were stored in museum conditions the major change that can be anticipated in these salts would be the dehydration of calcium acetate monohydrate to the hemihydrate as discussed in the following section.

Discussion

Regarding the source of the calclacite components, calcium undoubtedly derives from the calcareous component of the ceramic as either calcareous clay (Fillieries et al., 1983) or calcite inclusions (Rotroff, 2006) or both. NAA determined that a group of Subgeometric ceramics (750–650 BCE) in the Athenian Agora was constructed from calcareous clay (Fillieries et al., 1983). The main mineral components of Athenian Agora pottery have been

characterized as predominantly feldspar (some feldspars such as anorthite are calcium-rich) and quartz (Farnsworth, 1964) and quartz was identified as an inclusion in Hellenistic pottery by Raman laser microprobe (RLM) spectroscopy (Rotroff, 2006). The prevalence of calcite temper in the Hellenistic pottery of the Athenian Agora has been confirmed by RLM spectroscopy (Rotroff, 2006) that has provoked 'lime popping' in some vessels (Paterakis, 2013). Calcite decomposes during firing, forming lime that expands upon absorption of moisture, causing spalling ('lime popping') (Rice, 1987). Abundant evidence of this phenomenon is present in the pottery collection of the Athenian Agora (Paterakis, 2013).

Chloride may derive from cleaning with hydrochloric acid, as previously discussed (Koob, 2013), from saline soil during burial (Paterakis, 1998a), or from salt added to the clay before firing (Rotroff, 2006). During excavation of one quadrant of section BZ in the Athenian Agora chlorides in the soil were measured to a maximum concentration of 45 ppm with Hach Quantab® Chloride Titrator strips, using a weight-to-volume ratio of 1 g: 15 ml (soil weight to water volume) (Paterakis, 1998b). Groundwater chlorides can accumulate through continuous infiltration of water and evaporation, reaching salt concentrations greater than that found during this isolated test and sufficient to contribute to the formation of calclacite. Rotroff considers the intentional addition of salt to the clay to reduce the deleterious effects of the 'lime popping' to be a distinct possibility in Hellenistic pottery, judging by the coloration of the fabric (Rotroff, 2006). Sodium was determined to be prominent in the Hellenistic water jugs of the Athenian Agora by instrumental NAA (Rotroff, 2006). Chlorides may also derive from hydrochloric acid: the use of a 20% solution of hydrochloric acid to clean pottery by archaeologists in the Mediterranean world in the first half of the twentieth century is common knowledge (Dowman, 1970). Reference to the use of hydrochloric acid as a cleaning agent for ceramics in the Athenian Agora was published for Mycenaean pottery in 1966 (Farnsworth & Immerwahr, 1966). This practice was discontinued in 1979 with the appointment of the first professional conservation staff (Koob, 2013).

Acetate is known to result from the reaction of acetic acid emissions from wooden storage materials with the object, and the presence of soluble salts in the pores and on the surface of the ceramic encourages the reaction (Gibson et al., 2005). This was confirmed with accelerated efflorescence testing described in the introduction: efflorescence testing confirmed the contribution of a calcium component to the formation of calcium acetate when calcareous ceramic was
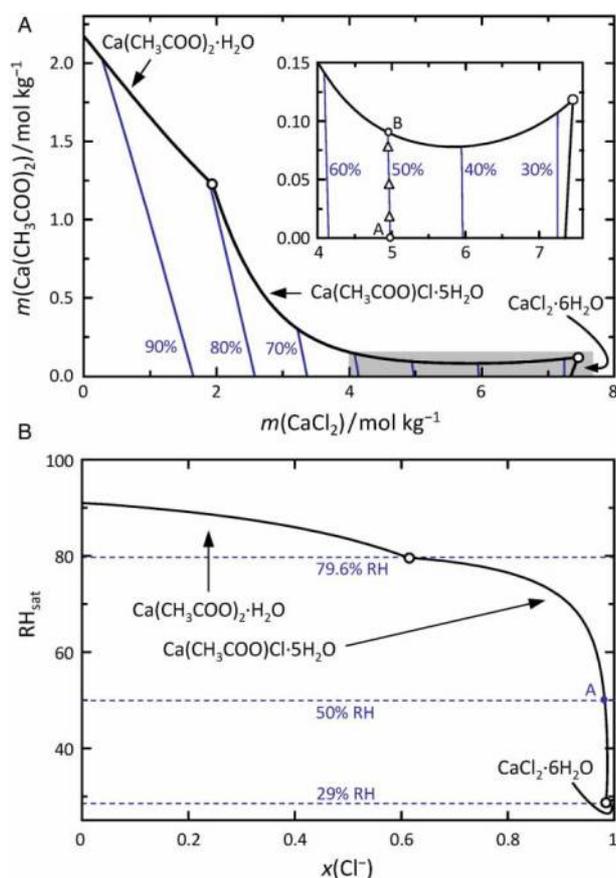
Figure 4 Phase diagram of the Ca(CH₃COO)₂–CaCl₂–H₂O system at 25°C. (A) Solubility diagram with stable phases calcium acetate hydrate, calclacite, and calcium chloride hexahydrate (inset gives enlarged view of shaded area with solubilities at high CaCl₂ concentration, blue lines are isolines of RH_eq); (B) RH deliquescence diagram for mixed solutions saturated with calclacite, calcium acetate hydrate, and calcium choride hexahydrate. The lines give the RH_sat below which a CaCl₂–Ca(CH₃COO)₂ mixed solution of a given mixing ratio (given as mole fraction chloride) should precipitate either calcium acetate hydrate, calclacite, or calcium chloride hexahydrate.

exposed to volatile acetic acid (Paterakis, 1995). Volatile acetic acid concentrations in wooden storage cases in the Athenian Agora collection have been found to range from 1039 ± 20 to $1267 \pm 20 \, \mu g/m^3$ (400 to 500 ppb) at 25°C (Paterakis, 2003). Similar concentrations have been identified in other collections in which acetate efflorescence has been identified on ceramics (Gibson & Watt, 2010).

The RH_eq is the relative humidity (RH) of air that is in equilibrium with a salt solution of a given composition. The RH that functions as the line of demarcation between the precipitation (crystallization) and dissolution (deliquescence) of a salt compound is termed the RH deliquescence (RH_del) or the equilibrium RH of the saturated solution (RH_sat). Described in another way, precipitation of salt depends on the presence of a saturated salt solution and a RH that will support the solid phase formation

(Gibson & Watt, 2010). Mixtures of salts will deliquesce within a range of RHs. For example, the RH_sat for the salt contaminants in the Athenian Agora was determined to range from 79 to 84% RH (Paterakis, 1999). The occurrence of precipitation resulting in efflorescence will be dictated by the composition of the salt solution in relation to its RH_sat and, therefore, control of the ambient RH may be a means with which to protect objects from the deliquescence-crystallization cycle. The success of preventive conservation and control in a collection will be determined, in part, by the feasibility of maintaining the target RH that will prevent this change in liquid-solid state. It has been shown that the attempt to render innocuous a salt that is commonly found in museum collections, namely thecotrichite ($Ca_3(CH_3COO)_3Cl(NO_3)_2 \cdot 7H_2O$), by controlling the RH is not a straightforward matter since the hygroscopic components, calcium chloride, and calcium nitrate, are active in RH levels as low as 20% (Gibson *et al.*, 2005).

A solubility diagram and a RH deliquescence diagram for mixed salt solutions containing calcium acetate and calcium chloride are depicted in Fig. 4. The diagrams have been calculated using a thermodynamic model of the $Na^+–Ca_2^+–Cl^-–CH_3COO^-–H_2O$ system (Steiger *et al.*, 2000). Although the ternary system Ca(CH₃COO)₂–CaCl₂–H₂O consists of only one cation (calcium) and two anions (chloride and acetate), it is a complex system due to the fact that both single salts can exist in different hydrated states. In addition, several double salts are known. However, at temperatures close to room temperature the only stable salts are $Ca(CH_3COO)_2 \cdot H_2O$ (calcium acetate monohydrate), $CaCl_2 \cdot 6H_2O$ (calcium chloride hexahydrate), and $Ca(CH_3COO)Cl \cdot 5H_2O$ (calclacite).

Calcium chloride hexahydrate is a very hygroscopic salt, its deliquescence humidity is only 29.3% at 25°C (Fig. 4B). At this humidity, the dry salt picks up moisture and forms a saturated solution. At higher RHs, the water uptake continues and the solution becomes more dilute. This is illustrated by the blue lines of RH_eq in the solubility diagram in Fig. 4A. At RHs above the RH_eq, the solution picks up moisture until it is in equilibrium again (now at the higher RH_eq). At humidities below the RH_eq, water evaporates from a solution. The lowest RH at which a solution can still exist is the saturation (or deliquescence) humidity RH_sat, i.e. the equilibrium humidity of the saturated solution. Below the RH_sat the salt crystallizes out. The saturation humidities of the mixed solutions are shown in Fig. 4B. It is obvious that $Ca(CH_3COO)_2 \cdot H_2O$ (RH_sat = 91.6%) is much less hygroscopic than $CaCl_2 \cdot 6H_2O$. In effect, the hygroscopicity of mixtures of the two salts is largely controlled by the calcium chloride concentration; low equilibrium humidities

require high calcium chloride concentrations. The blue lines give the compositions of mixed solutions that are in equilibrium with 90, 80, 70, 60, 50, 40, and 30% RH (the last four only labeled in the inset). The inset in Fig. 4A shows an enlarged view of the diagram at high calcium chloride concentrations. The intersections of these lines with the solubility curves yield the composition of the saturated solutions at 90%, 80% etc. These values are plotted in Fig. 4B as RH_{sat} (RH_{eq} of saturated solutions). The composition is expressed as mole fraction chloride ($Cl^-/(Cl^- + CH_3COO^-)$). The intersections of these lines with the x-axis give the concentrations of pure $CaCl_2$ solutions ($Ca(CH_3COO)_2 = 0$) that are in equilibrium with RH 90%, 80% etc. of the surrounding air. It can be seen that the concentration decreases from 7.4 mol/kg at saturation ($RH_{sat} = 29.3\%$) to about 5 mol/kg at 50% RH. In other words, if a 5 mol/kg $CaCl_2$ solution is exposed at 50% RH, nothing happens (this is point A in the inset). If the same solution is exposed to 30% RH, water evaporates and the solution becomes more concentrated (about 7.2 mol/kg, the intersection of the 30% line with the x-axis). No crystallization would occur as the RH is still above the deliquescence (or saturation humidity) of 29%. If the 5 mol/kg solution is exposed to 60% RH, it will pick up moisture and become more dilute (i.e. about 4.2 mol/kg, i.e. the RH_{eq} of a 4.2 mol/kg solution is 60%). Hence, in a typical museum atmosphere, calcium chloride in an object is always present as a concentrated 5 molal solution (see inset of Fig. 4A). In contrast, pure calcium acetate will be present in crystalline form at all times under such conditions. The double salt calclacite can crystallize from mixed solutions of the two salts in the humidity range from 29 to 79.6% RH (Fig. 4B).

In the case of the Athenian Agora and all pottery collections with salt contamination issues, ideally the salt contaminants should be identified and the RH_{sat} of the salt mixtures characterized in order to determine the appropriate RH levels for the safe storage of the ceramics collection (Paterakis & Nunberg, 1996). Regarding salt identification, it has been shown that sampling the crystallization on the surface is not adequate for a comprehensive determination. Salts in the body can differ in composition from those on the surface as has been shown in the case of thecotrichite ($Ca_3(CH_3COO)_3Cl(NO_3)_2·7H_2O$) on glazed tiles (Linnow *et al*., 2007). Salts in the body may be extracted through desalination and analyzed by ion chromatography, among other methods. Destructive sampling of the ceramic to carry out a qualitative and quantitative analysis of salts through a cross section of the body is another option (Gibson *et al*., 2005). In the case of thecotrichite, it was determined that acetate was present in the crystals on the surface but not in the body of the

ceramic (Linnow *et al*., 2007). The highly soluble calcium nitrate and calcium chloride were found in the body that reacted with volatile acetic acid emissions forming crystallization of thecotrichite on the surface of the ceramic (Linnow *et al*., 2007). In the case of thecotrichite it was found that maintenance of crystals on the surface of an object does not guarantee stability and protection to the object (Gibson *et al*., 2005). At typical museum conditions (about 55% RH) thecotrichite can crystallize out while the hygroscopic salts, calcium nitrate, and calcium chloride in the pores promote further dissolution of acetic acid, serving as a reservoir for more thecotrichite crystallization and continued deterioration of the object. Thecotrichite derives from a complex quaternary system consisting of one cation (calcium) and three anions (chloride, nitrate, and acetate) that contribute to its complicated crystallization-deliquescence behavior. A phase diagram has been developed for thecotrichite that may be used to determine which solid phase or phases 'would precipitate out from a mixed solution of any given composition' (Gibson *et al*., 2005, p. 289). Phase transitions and the kinetics of crystal growth depend on '(1) composition of the salt mixture, (2) degree of disparity between ambient conditions and equilibrium conditions, (3) air movement, and (4) characteristics of the porous material' (Price, 2000, p. 10).

It is conceivable that a similar mode of formation may occur with calclacite, i.e. soluble calcium chloride salts in the body react with acetic acid emissions on the surface causing crystallization of calclacite, and that a much higher concentration of acetate may be found on the surface than in the pores of the object. Assuming that cleaning with hydrochloric acid is in fact the major source of chloride in the Athenian Agora pottery, calcium chloride is formed by reaction of hydrochloric acid with the calcite ($CaCO_3$) present in the ceramics. As discussed before and illustrated in Fig. 4A, the calcium chloride is present in the ceramics as a rather concentrated (5 molal) solution at 50% RH (point A in the inset of Fig. 4A). If such an object is exposed to a contaminated atmosphere, the calcium chloride solution provides an ideal sink and picks up acetic acid vapor resulting in a decrease in the pH of the solution. The acidity formed is neutralized by dissolution of calcite and formation of calcium acetate. Continuous deposition of acetic acid, thus, leads to a continuous increase of the calcium acetate concentration. Then, the solution composition follows the arrows along the 50% RH isoline in the inset of Fig. 4A. However, due to the low solubility of calclacite at such high chloride concentration, saturation with calclacite is reached quickly at point B. Any further deposition of acetic acid and formation of calcium acetate will then cause the crystallization of calclacite. Crystal growth occurs preferably close to

the surface where the acetic acid is deposited from the surrounding atmosphere. This may simply lead to the formation of an efflorescence on the surface, or, a growing crystal may become confined in a pore close to the surface. In the latter case, the growing crystal can generate stresses that are sufficient to cause damage, i.e. the formation of cracks or granular disaggregation.

Although the crystallization of calclacite consumes part of the chloride that is present, the calcium concentration in the solution remains constant as long as the RH is constant. In principle, the reaction proceeds until all chloride is consumed. Once all chloride is consumed further acetic acid deposition leads to the formation of calcium acetate. If the concentration of calcium chloride is small, the amount of calclacite formed is also small. It should be emphasized that the formation of calclacite is dependent on the presence of chloride just as the formation of thecotrichite is dependent on the presence of nitrate and chloride. There is also no chloride threshold concentration, as long as chloride and acetate are present calclacite can be precipitated. In the absence of chloride and nitrate, calcium acetate will form (the hemihydrate in normal ambient conditions). This was confirmed by efflorescence tests in which calcareous ceramic exposed to volatile acetic acid formed calcium acetate crystallization (Paterakis, 1995).

This analogy of thecotrichite and calclacite formation may account for the presence of different salt morphologies of Agora sample 3 observed in the ESEM according to location (surface, under the glaze, in the pores) and the predominance of calclacite on the surface. The salt crystals visible in ESEM under the surface and in the pores could be chloride salts, whereas calclacite was identified predominantly on the surface by XRD and PLM. Calcium chloride was detected as a trace in sample 11, supporting this theory. There are different possible pathways of calcium acetate hemihydrate formation, which was found as a minor compound in the efflorescence on a few samples. This is in accordance with the solubility diagram, which predicts that calcium acetate hydrate can only precipitate from the mixed solution at high RH, namely above the monohydrate-calclacite transition (79.6% at 25°C, Fig. 4B). Minor amounts of calcium acetate hydrate may also be formed by direct reaction of acetic acid vapor with $CaCO_3$ in absence of a $CaCl_2$-containing solution. Moreover, as can be seen from Fig. 4A, small amounts of calcium acetate monohydrate might co-precipitate with calclacite from the mixed solution. This is because the solubility of the monohydrate, as estimated by extrapolation of the monohydrate branch in the solubility diagram, is probably not much higher than the calclacite solubility. Finally, it is also plausible that calcium acetate was identified as the hemihydrate. Even if the monohydrate is formed initially, it dehydrates to the hemihydrate below 67–71% RH at 20–25°C (Fig. 5). Normal museum conditions (about 55% RH) in which the salts were stored and underwent analysis supported the hemihydrate.

Conclusions

The proposed mode of formation of calclacite on $CaCl_2$-containing objects that are exposed to acetic acid vapor is in agreement with the experimental results. It is predicted that calclacite is formed as the major compound under typical museum conditions and should be preferably precipitated close to the surface of an object.

Desalination successfully removes chloride contaminants from burial and chloride residues from acid cleaning as well as efflorescing salts. Desalination eliminates any possible recontamination by removing both the free calcium and chloride ions. Those ceramics in the Agora that have been desalinated since 1979 have remained stable without subsequent efflorescence formation. Since some acetate compounds, such as calcium acetate hemihydrate, can form without the presence of chloride in wooden cases, ceramics should not be stored in wood as a general rule. It is recommended that the wooden storage cases in the Agora be replaced with enameled steel cases to prevent the formation of acetate salts. This would be an expensive undertaking given the large size of the ceramics collection (52,000 objects). Another means
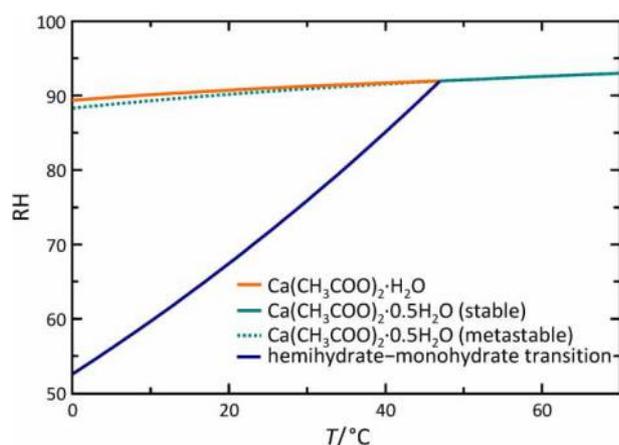
Figure 5   Deliquescence diagram according to RH and temperature shows the deliquescence humidities of calcium acetate hemihydrate and calcium acetate monohydrate and also the hydration-dehydration equilibrium curve. The green dotted curve is the deliquescence humidity of the hemihydrate at low temperatures, i.e. where the monohydrate is the stable phase. At lower RH calcium acetate monohydrate is dehydrated to the hemihydrate (67–71% RH at 20–25°C). Both salts have very similar deliquescence humidities.

to prevent salt formation is through control of the RH and temperature. In this case the same formidable economic constraints apply given the large area of the storerooms. Sealing the internal surfaces of the wooden cases with impermeable barriers such as Marvelseal® is another option that would require considerable man hours and expense.

The pottery in this study was exposed to volatile acetic acid emissions in storage for decades. The goal of conservation is to prevent acetic acid contamination by using appropriate conservation treatments and storage materials and by improving the climatic conditions. Every collection requires careful characterization to determine whether the deleterious effects of salt contaminants may be controlled by RH regulation.

As this study has shown, the identification of complex salt compounds presents many difficulties, not the least of which include the potential transformation of salt composition and state of hydration during storage, handling, and analysis. Ideally, the salts should be analyzed immediately upon sampling and the same crystals used first for XRD and then for PLM. The salts should not be exposed to purge gas or vacuum during XRD or SEM. Salt samples should be protected from fluctuations in temperature and RH that can cause alteration in the crystals.

Acknowledgments

References

Arnold, A. & Zehnder, K. 1991. Monitoring Wall Paintings Affected by Soluble Salts. In: S. Cather, ed. *The Conservation of Wall Paintings, Proceedings of a Symposium Organized by the Courtauld Institute of Art and the Getty Conservation Institute, London, July 13–16, 1987*. Los Angeles: The Getty Conservation Institute, pp. 103–35.

Byne, L.S. 1899. The Corrosion of Shells in Cabinets. *Journal of Conchology*, 9: 253–54.

Doehne, E. 1994. Electron Microscopy Report. Los Angeles: The Getty Conservation Institute, unpublished report.

Dowman, E.A. 1970. *Conservation in Field Archaeology*. London: Methuen.

Farnsworth, M. 1964. Greek Pottery: A Mineralogical Study. *American Journal of Archaeology*, 68(3): 221–28.

Farnsworth, M. & Immerwahr, S.A. 1966. The Use of Tin on Mycenaean Vases. *Hesperia: The Journal of the American School of Classical Studies at Athens*, 35: 381–96.

Fillieries, D., Harbottle, G. & Sayre, E.V. 1983. Neutron-activation Study of Figurines, Pottery, and Workshop Materials from the Athenian Agora, Greece. *Journal of Field Archaeology*, 10: 55–69.

FitzHugh, E.W. & Gettens, R.J. 1971. Calclacite and Other Efflorescent Salts on Objects Stored in Wooden Museum Cases. In: R. Brill, ed. *Science and Archaeology*. Cambridge: MIT Press, pp. 91–102.

Gibson, L.T., Cooksey, B.G., Littlejohn, D., Linnow, K., Steiger, M. & Tennent, N.H. 2005. The Mode of Formation of Thecotrichite, a Widespread Calcium Acetate Chloride Nitrate Efflorescence. *Studies in Conservation*, 50(4): 284–94.

Gibson, L.T. & Watt, C.M. 2010. Acetic and Formic Acids Emitted from Wood Samples and their Effect on Selected Materials in Museum Environments. *Corrosion Science*, 52: 172–78.

Halsberghe, L., Gibson, L.T. & Erhardt, D. 2005a. A Collection of Ceramics Damaged by Acetate Salts: Conservation and Investigation into the Causes. In: I. Verger, ed. *ICOM Committee for Conservation, 14th triennial Meeting, Preprints*. London: Earthscan Ltd., pp. 131–38.

Halsberghe, L., Erhardt, D., Gibson, L.T. & Zehnder, K. 2005b. Simple Methods for the Identification of Acetate Salts on Museum Objects. In: I. Verger, ed. *ICOM Committee for Conservation, 14th Triennial Meeting, Preprints*. London: Earthscan Ltd., pp. 639–47.

Koob, S.P. 1986. The Use of Paraloid B-72 as an Adhesive: Its Application for Archaeological Ceramics and Other Materials. *Studies in Conservation*, 31: 7–14.

Koob, S.P. 2013. [Personal communication]. Corning, NY: Corning Museum of Glass.

Linnow, K., Halsberghe, L. & Steiger, M. 2007. Analysis of Calcium Acetate Efflorescences Formed on Ceramic Tiles in a Museum Environment. *Journal of Cultural Heritage*, 8: 44–52.

Mau, L. 1992. Salt Efflorescence on Greek Pottery from the Agora Excavation. Malibu: J. Paul Getty Antiquities Laboratory, unpublished report.

Paterakis, A.B. 1990. A Preliminary Study of Salt Efflorescence in the Collection of the Ancient Agora, Athens, Greece. In: K. Grimstad, ed. *ICOM Committee for Conservation, 9th Triennial Meeting, Preprints*. Los Angeles: ICOM, pp. 675–79.

Paterakis, A.B. 1992. The Consolidation and Desalination of Ceramic Impregnated with Sodium Sulphate. In: P.B. Vandiver, J.R. Druzik, G.S. Wheeler & I.C. Freestone, eds. *Materials Issues in Art and Archaeology III, Materials Research Society Symposium Proceedings No. 267*. Pittsburgh: Materials Research Society, pp. 1071–76.

Paterakis, A.B. 1993. The Consolidation and Desalination of Ceramic Impregnated with Calcium Acetate. In: J. Bridgland, ed. *Preprints of the ICOM Committee for Conservation 10th Triennial Meeting, Washington DC*. Los Angeles: ICOM Committee for Conservation, pp. 704–08.

Paterakis, A.B. 1995. Efflorescence Testing of Pottery. In: P. Vincenzini, ed. *The Ceramics Cultural Heritage*. Faenza: Techna srl, pp. 661–68.

Paterakis, A.B. & Nunberg, S. 1996. The Stabilization of Archaeological Pottery in an Excavation Study Collection through Relative Humidity Control and through Desalination. In: M. Stefanaggi, ed. *Le Dessalement des Matériaux Poreux, 7es Journées d'études de la SFIIC*. Champs-sur-Marne: SFIIC, pp. 137–44.

Paterakis, A.B. 1998a. The Desalination of Consolidated Ceramics. In: A.B. Paterakis, ed. *Glass, Ceramics and Related Materials, Preprints of the ICOM Committee for Conservation Working Group 'Glass, Ceramics and Related Materials' Interim Meeting*. Helsinki: EVTEK – Institute of Arts & Design, pp. 144–53.

Paterakis, A.B. 1998b. Soil Analysis in the Athenian Agora. Athens: American School of Classical Studies, unpublished report.

Paterakis, A.B. 1999. Those Evasive Salt Crystals. In: J. Bridgland, ed. *ICOM Committee for Conservation, 12th Triennial Meeting, Preprints*. London: James & James (Science Publishers) Ltd, pp. 799–802.

Paterakis, A.B. 2003. The Influence of Conservation Treatments and Environmental Storage Factors on Corrosion of Copper Alloys in the Ancient Athenian Agora. *Journal of the American Institute for Conservation*, 42: 313–39.

Paterakis, A.B. 2013. Unpublished observations made and knowledge acquired while serving as Head of Conservation, Athenian Agora Excavations, American School of Classical Studies, Athens, Greece.

C. Price, ed. 2000. *An Expert Chemical Model for Determining the Environmental Conditions Needed to Prevent Salt Damage in Porous Materials*. Protection and Conservation of the European Cultural Heritage, Project ENV4-CT95–0135 (1996–2000) Research Report No 11, European Commission Directorate-General Science, Research and Development. London: Archetype Publications, Ltd.

Rice, P.M. 1987. *Pottery Analysis: A Sourcebook*. Chicago: University of Chicago Press.

Robinet, L., Eremin, K., Cobo del Arco, B. & Gibson, L.T. 2004. A Raman Spectroscopic Study of Pollution-induced Glass Deterioration. *Journal of Raman Spectroscopy*, 35: 662–70.

Rotroff, S. 2006. Hellenistic Pottery: The Plain Wares. *The Athenian Agora*, 33: iii–iv, vii–ix, xi–xxi, xxiii–xxxvii, 1, 3–53, 55–67, 69–223, 225–39, 241, 243–337, 339, 341–77, 379–91, 393–99, 401–03, 405–07, 409–29, 431–38.

Scott, A. 1926. *The Cleaning and Restoration of Museum Exhibits, Third Report*. London: H.M.S.O.

Stahlbuhk, A. 2012. Analyse von Calciumacetat-Ausblühungen auf Museumsexponaten (Analysis of Calcium Acetate Efflorescences on Museum Artifacts). BA Thesis, Universität Hamburg, Germany.

Steiger, M., Beyer, R. & Dorn, J.A. 2000. Thermodynamic Model of the Na^+–$Ca2^+$–Cl–CH_3COO–H_2O System. In: C. Price, ed. *An Expert Chemical Model for Determining the Environmental Conditions Needed to Prevent Salt Damage in Porous Materials*, Protection and Conservation of the European Cultural Heritage Project ENV4-CT95-0135 (1996-2000) Research Report No 11, European Commission Directorate-General Science, Research and Development. London: Archetype Publications, Ltd., pp. 45–52.

Taboury, K.F. 1931. Des modifications chimiques de certaines substances calcaires conservees dans des meubles en bois. *Bulletin de la Société Chimique de France*, 49: 1289–93.

Van Tasssel, R., 1945. Une Efflorescence d'Acetatochlorure de Calcium sur des Roches Calcaires dans des Collections. *Bulletin du Musee royal d'Histoire naturelle de Belgique*, 21, 26 (Dec.), Brussels.

Van Tassel, R. 1958. On the Crystallography of Calclacite, $Ca(CH_3COO)Cl \cdot 5H_2O$. *Acta Crystallographica*, 11: 745–46.

Wheeler, G.S. & Wypyski, M.T. 1993. An Unusual Efflorescence on Greek Ceramics. *Studies in Conservation*, 38: 55–62.

Zehnder, K. & Arnold, A. 1989. Crystal Growth in Salt Efflorescence. *Journal of Crystal Growth*, 97: 513–21.